Biomedicine & Pharmacotherapy 152 (2022) 113240

Contents lists available at ScienceDirect

Biomedicine & Pharmacotherapy

journal homepage: www.elsevier.com/locate/biopha

# FTY720 decreases ceramides levels in the brain and prevents memory impairments in a mouse model of familial Alzheimer's disease expressing APOE4

Simone M. Crivelli [a,b,1,2], Qian Luo [a,2,3], Daan van Kruining [a], Caterina Giovagnoni [a], Marina Mané-Damas [a], Sandra den Hoedt [c], Dusan Berkes [d], Helga E. De Vries [e], Monique T. Mulder [c], Jochen Walter [f], Etienne Waelkens [g], Rita Derua [g], Johannes V. Swinnen [h], Jonas Dehairs [h], Erwin P.M. Wijnands [i], Erhard Bieberich [b,j], Mario Losen [a], Pilar Martinez-Martinez [a,*]

[a] Maastricht University, Department of Psychiatry and Neuropsychology, School for Mental Health and Neuroscience, Maastricht 6200MD, the Netherlands
[b] Department of Physiology, University of Kentucky College of Medicine, Lexington 40506, KY, USA
[c] Department of Internal Medicine, Laboratory Vascular Medicine, Erasmus MC University Medical Center, Rotterdam 3000CA, the Netherlands
[d] Department of Organic Chemistry, Slovak University of Technology, Radlinského 9, 81237 Bratislava, Slovak Republic
[e] Department of Molecular Cell Biology and Immunology, Amsterdam Neuroscience, Amsterdam UMC, Amsterdam 1007MB, the Netherlands
[f] Department of Neurology, University Hospital Bonn, University of Bonn, Bonn D-53127, Germany
[g] Laboratory of Protein Phosphorylation and Proteomics, KU Leuven, Leuven 3000, Belgium
[h] Laboratory of Lipid Metabolism and Cancer, KU Leuven, Leuven 3000, Belgium
[i] Department of Pathology, Maastricht University, Maastricht 6200MD, the Netherlands
[j] Veterans Affairs Medical Center, Lexington, KY 40502, USA

ARTICLE INFO

*Keywords:*
FTY720
S1P
Ceramide
Sphingomyelin
APOE4
APOE3
5xFAD
Memory
Anxiety

ABSTRACT

The protection mediated by the bioactive sphingolipid sphingosine-1-phosphate (S1P) declines during Alzheimer's disease (AD) progression, especially in patients carrying the apolipoprotein E ε4 (APOE4) isoform. The drug FTY720 mimics S1P bioactivity, but its efficacy in treating AD is unclear. Two doses of FTY720 (0.1 mg / kg and 0.5 mg / kg daily) were given by oral gavage for 15 weeks to transgenic mouse models of familial AD carrying human apolipoprotein E (APOE) APOE3 (E3FAD) or APOE4 (E4FAD). After 12 weeks of treatment, animals were subjected to behavioral tests for memory, locomotion, and anxiety. Blood was withdrawn at different time points and brains were collected for sphingolipids analysis by mass spectrometry, gene expression by RT-PCR and Aβ quantification by ELISA. We discovered that low levels of S1P in the plasma is associated with a higher probability of failing the memory test and that FTY720 prevents memory impairments in E4FAD. The beneficial effect of FTY720 was induced by a shift of the sphingolipid metabolism in the brain towards a lower production of toxic metabolites, like ceramide d18:1/16:0 and d18:1/22:0, and reduction of amyloid-β burden and inflammation. In conclusion, we provide further evidence of the druggability of the sphingolipid system in AD.

* Correspondence to: Department of Psychiatry and Neuropsychology, Maastricht University, Universiteitssingel 50, 6229ER Maastricht, the Netherlands.
*E-mail addresses:* s.crivelli@uky.edu (S.M. Crivelli), p.martinez@maastrichtuniversity.nl (P. Martinez-Martinez).
[1] **First author:** PhD Simone M. Crivelli; Department of Psychiatry and Neuropsychology; Maastricht University; Universiteitssingel 50; 6229 ER Maastricht, the Netherlands.
[2] equal contribution.
[3] Current location: Department of Neurosurgery & Pathophysiology, Institute of Neuroregeneration and Neurorehabilitation, Qingdao University, 308 Ningxia Street, Qingdao 266071, China.

https://doi.org/10.1016/j.biopha.2022.113240
Received 17 March 2022; Received in revised form 31 May 2022; Accepted 2 June 2022
Available online 9 June 2022

## 1. Introduction

Alzheimer's disease (AD) is a multifactorial neurodegenerative disorder neuropathologically characterized by extracellular amyloid-β (Aβ) aggregates visualized as plaques and intracellular neurofibrillary tangles (NFT) composed by hyper-phosphorylated tau [1–3]. Synaptic dysfunction and progressive neurodegeneration in specific brain regions leads to learning and memory impairment and changes in emotional behavior [4].

Sphingolipids, like ceramide (Cer) or sphingosine 1-phosphate (S1P), are structurally diverse lipids that are essential membrane constituents and potent bioactive molecules that have been associated to onset and progression of AD [5]. During AD pathophysiology, a metabolic shift favoring the production of Cer over S1P synthesis in the brain contributes to Aβ plaque formation, neuroinflammation and neuronal apoptosis [6–8]. On one hand, the enzymes involved in Cer production like serine palmitoyl-transferase, ceramide synthases (1, 2 and 6) and sphingomyelinases are upregulated in AD brains [9–11]. On the other hand, the enzymes synthesizing or breaking down S1P are down or upregulated, respectively [12,13]. The consequence of this metabolic shift is believed to be threefold: first, pro-apoptotic signaling mediated by Cer is increased while neuroprotective S1P is reduced, compromising neuronal homeostasis [14–17]; second, Cer potentiates and stabilizes the proteolytic enzymes β and γ secretase which produces Aβ [18–20]; third, Cer itself or more complex downstream products like glycoceramides are found in Aβ plaques and trigger aggregation and toxicity of Aβ [8, 21–23]. Therefore, pharmacological modulation of Cer and S1P metabolism may impact Aβ pathology.

FTY720, also known as Fingolimod, is a sphingosine analog with a potent immunosuppressive activity [24]. To exert its immunosuppressive activity, the drug requires to be phosphorylated in vivo by the sphingosine kinase (SPHK) to form the active moiety [25]. FTY720, once phosphorylated, binds to S1P receptors causing internalization and degradation of the receptor, causing primarily lymphopenia in vivo [25]. Interestingly, in vitro and in vivo data suggest that FTY720 are modulators of Aβ production independently from S1P receptors activation [26,27]. Cell-based assays demonstrated that FTY720 reduced γ-secretase-mediated cleavage of amyloid precursor protein (APP) thus attenuating Aβ release in the medium [26]. Furthermore, intraperitoneal injection of FTY720 for 6 days protected from Aβ-induced memory impairment and neural damage [28]. In alignment with this, Fukumoto et al. found that oral administration of FTY720 ameliorated memory impairment and associative learning in mice injected with amyloid peptides [29]. In 3-month-old 5xFAD mice, which is a severe model of familial AD, FTY720 decreased Aβ plaque density in the brain, as well as soluble and insoluble Aβ measured by enzyme-linked immunosorbent assay [30]. Furthermore, FTY720 decreased astrocytic activation, marked by glial fibrillary acidic protein (GFAP) staining, and the number of activated microglia [30]. Van Doorn et al. also reported the protective action of FTY720 on Cer induced brain endothelial barrier alterations [31]. Hence, we hypothesize that FTY720 administration could have a fourfold beneficial effect in transgenic mice models of FAD, (i) restore the sphingolipid misbalance typical of AD, (ii) ameliorate Aβ pathology, (iii) attenuate neuroinflammation (iiii) and improve thereby memory impairments. The drug was tested on E3FAD and E4FAD transgenic mice generated by crossbreeding the 5xFAD with human APOE3 or APOE4 replacement mice [32]. These transgenic models were selected to address APOE4 impact on S1P metabolism since it has been reported that S1P neuroprotection declines during AD progression, especially in patients carrying the apolipoprotein E ε4 (APOE4) isoform [12].

## 2. Materials and methods

### 2.1. Drug preparation

The drug FTY720 was kindly provided by Barbara Nuesslein-Hildesheim, Novartis Pharma AG Basel, Switzerland in powder form. A stock of FTY720 (FTY720 1 mg / mL in water) was prepared every two weeks and stored at 4 °C. For daily administration by oral gavage, the final dosing concentrations were prepared by diluting the stock in water and used for a maximum of one week and stored at 4 °C. In this study, two doses were tested: a high dose (0.5 mg / kg / day) and a low dose (0.1 mg / kg / day); water was given to the control groups. Experimenters administering the drug and performing behavior experiments were kept blinded for the treatment and genotype throughout the study.

### 2.2. Animals

E3FAD, E4FAD (FAD group) and APOE3, APOE4 (Control littermates) were purchased from Dr. Mary Jo LaDu (University of Illinois at Chicago) and bred in-house as previously explained [32]. Female mice used in this study were housed socially on a reverse 12-h day-night cycle and had ad libitum access to food and water. Female mice were selected because of the more severe disease progression compared to males [33]. The drug was given by oral gavage starting at the age of 12 weeks and lasted for 15 weeks. Behavior testing started after 12 weeks of drug administration when the animals were 24–25 weeks old. Blood was withdrawn starting from 10 weeks of age every 2 weeks alternating leg and stopped three weeks before the starting of the behavioral text. The animal numbers of the study are reported in Table S1. After 15 weeks of treatment, the animals were euthanized by an overdose of pentobarbital, and blood was immediately withdrawn and the animals perfused with Tyrode's solution. The two hemispheres of the brain were separated, and one half was micro-dissected into the brain stem, and cortex and snap-frozen in liquid nitrogen. The cortex was then powdered in iron mortar partly emerged in liquid nitrogen, aliquoted and weighted. The other half was fixed in 4% paraformaldehyde (PF) and moved into 30% sucrose in 0.1 M phosphate buffer saline (PBS) before freezing the tissue in an embedding medium. Alternatively, mice were perfused with 4% PF and processed as previously described [34].

### 2.3. Behavioral procedures

The Water maze (WM) was performed to assess spatial memory as previously described [35–37]. In brief, animals were placed in a water tank which consists of a circular black tub (Material: polyethylene; dimensions: diameter 81 cm) filled with clear tap water at a temperature of approximately 25 °C and challenged to escape through a hidden platform consisting of a black polyethylene cylinder (diameter 5 cm) which was submerged 0.5 cm below the surface of the water. Initially, mice were trained to find the platform over 4 trials/day (10-min intertrial interval, maximum trial duration of 60 s, with 3 s on the platform at the end of each trial) for four days. Animals that failed to find the platform within 60 s were placed on the platform for about 3 s. Finally, a probe trial was given 24 h after the last training trial. In the probe trial, the platform was removed, and the latency to the platform area and the time spent in the target quadrant (quadrant where platform was hidden) was measured with a tracking system (Ethovision Pro, Noldus Information Technology).

The Y-maze spontaneous alternation (AYM) was conducted as previously described [34]. The number of arm entries and the number of triads were recorded to calculate the percentage of alternations.

The Open field (OF) task was performed as described elsewhere [38]. Briefly, locomotion activity was assessed in a square divided into 4 equal arenas. At the start of a trial, the animals were placed in the center of each arena. The total distance traveled was measured under low light conditions by a video camera connected to a video tracking system

(Ethovision Pro, Noldus Information Technology).

The Elevated zero-maze (EZM) was conducted as previously described [34]. The total and relative duration and distance traveled in the open and enclosed arms were measured in the dark via an infrared video camera connected to a video tracking system (Ethovision Pro, Noldus Information Technology).

### 2.4. Lipidomics analysis

Powder aliquots of cortex were homogenized with a Precellys 24 Tissue Homogenizer in 800 μL of water, of which 700 μL was used for lipid extraction. Extraction and lipidomics were carried out by Lipometrix, the lipidomics core facility at KU Leuven, as described [39]. Lipid data is expressed as relative percentage of the lipid family.

### 2.5. Sphingolipid analysis

Lipid extraction. Sphingolipids were extracted based on the Blight and Dyer method as previously described [34,40]. Powder aliquots of cortex were homogenized in cold purified Millipore water (MQ, 18.2 MΩ cm) from a Milli-Q® PF Plus system (Millipore B.V.). Total lipids were extracted from the weighted amount of tissue and plasma samples by adding methanol (MeOH), containing Cer-C17:0, Cer-C17:0/24:1, SM-C17 and S1P-D7 (2, 2, 10 and 0.2 μg/mL methanol; Avanti Polar Lipids) as internal standard, and 10% TEA solution (trimethylamine (10/90, v/v) in MeOH/dichloromethane (DCM) (50/50, v/v)). Subsequently, MeOH/DCM (50/50, v/v) was added to this mixture. Samples were vortexed and incubated under constant agitation for 30 min at 4 °C. After incubation, samples were centrifuged at 14,000 rpm for 20 min at 4 °C. The supernatant was transferred to a glass vial, dried under nitrogen, and reconstituted in MeOH before liquid chromatography-tandem mass spectrometry (LC-MSMS).

Protein content. The protein content of all brain region samples was determined by bicinchoninic acid assay (Thermo Fisher Scientific, Waltham, Massachusetts, USA) according to the manufacturer's instructions. An 8-point calibration curve was used to determine exact protein levels. Protein content was used to normalize brain sphingolipid levels for the actual input.

LC-MS/MS analysis. An autosampler (Shimadzu) injected 10 μL brain lipid extracts or 5 μL plasma lipid extracts into a Shimadzu HPLC system (Shimadzu) equipped with a Kinetex C8 column (50 ×2.1 mm, 2.6 μm, Phenomenex) at 30 °C using a gradient, starting from 95% mobile phase A (MQ/MeOH (50/50, v/v) containing 1.5 mM ammonium formate and 0.1% formic acid) for 2 min and increased to 93% mobile phase B (100% MeOH containing 1 mM ammonium formate and 0.1% formic acid) at 5.5 min. After 10 min, the column was flushed with 99% mobile phase B for 2 min before a 2-minute re-equilibration. The flow rate was set at 0.25 mL/min and the total run time was 14 min. The effluent was directed to a Sciex Qtrap 5500 quadruple mass spectrometer (AB Sciex Inc.) and analyzed in positive ion mode following electrospray ionization.

Nine-point calibration curves were constructed by plotting area under the curve, separately for Cers, S1P and SMs, for each calibration standard Cer d18:1/14:0, Cer d18:1/16:0, Cer d18:1/18:0, Cer d18:1/20:0, Cer d18:1/22:0, Cer d18:1/24:1, Cer d18:1/24:0, S1P, SM d18:1/16:0, SM d18:1/18:1, SM d18:1/18:0, SM d18:1/22:0, SM d18:1/24:1, SM d18:1/24:0 (Avanti polar lipids, Alabaster, AL, USA; SM-C20:0 and SM 18:1/22:0 Matreya LLC) normalized to the internal standard. Correlation coefficients (R2) obtained were $> 0.99$. Sphingolipid concentrations were determined by fitting the identified sphingolipid species to these standard curves based on acyl-chain length. Instrument control and quantitation of spectral data were performed using MultiQuant software (AB Sciex Inc.). Lipid data of the brain was expressed as pmol / mg tissue. Plasma data was expressed as pmol / mL for Cer and S1P or nmol / mL for SM.

### 2.6. Fluorescence-activated cell sorting (FACs)-analysis

Peripheral blood leukocytes, sorted and measured from blood samples, were collected at the end of the experiment as previously explained [41,42]. The complete FACs gating strategy is reported in Figure S1. Absolute circulating leukocyte subset numbers were determined by flow cytometry, calibrated using Trucount Beads (BD). Leukocytes were defined as CD45 + cells (clone 30 F-11, Biolegend).

### 2.7. FTY720 and FTY720-phosphorylated (FTY720-P) determination in plasma and brain

FTY720 and FTY720-P concentrations in plasma and brain were determined by UHPLC-MS-MS. From each blood sample, a 20 μL aliquot was transferred to Eppendorf tubes and diluted with 50% acetonitrile. Stable isotope labeled internal standards were added (10 μL c = 400 ng/mL) and proteins were precipitated by adding 280 μL of a solvent mixture containing 40% acetonitrile, 30% methanol and 30% trichloromethane. To spinal cord samples 20 μL 5% BSA in PBS, 10 μL internal standard, and 500 μL of the precipitation mix, described above, was added to homogenization tubes filled with ceramic beads of 1.4 mm diameter. Homogenization was performed with a Precellys 24 system. The stable isotope labeled internal standard was added to each calibration, quality control, and recovery control sample, except blank samples. After vortexing and sonication, the precipitated proteins and residuals were separated by centrifugation. The upper organic layer was transferred to Eppendorf tubes and evaporated to dryness using a SpeedVac concentrator. After per-acetylation with acetic anhydride in pyridine and after evaporation to dryness, the residues were dissolved in 60 μL methanol containing 0.2% formic acid by vortexing and sonication. After centrifugation, 55 μL of the supernatant was transferred to HPLC-μVials and held at 15 °C until analysis. For the quantitative determination, an Agilent 1290 UHPLC-system, directly coupled to the AP-ESI source of an Agilent 6490QQQ mass spectrometer. For separation, 5 μL of each sample was injected onto an Acquity UPLC BEH C18 2.1 × 50 mm column, held at 50 °C, and filled with 1.7 μm particles. A linear gradient from 50% B in A to 100% B within 4.5 min at a flow rate of 200 μL / min was applied. Solvent A was 5 mM ammonium acetate in water/acetonitrile/methanol 8/1/1, containing 0.02% acetic acid and B was acetonitrile/methanol 1:1 containing 0.02% acetic acid. For detection, the column effluent was directly guided to the electrospray source of the triple quadrupole MS with parameters optimized for FTY720-P. The FTY derivative was detected in positive mode, whereas for FTY-P derivative, the negative ion mode was selected, using the MRM transitions 434.3 $m/z > 255.1$ $m/z$, 374.2 $m/z$ for FTY, respectively 512.2 $m/z > 470.2$ $m/z$, 410.3 $m/z$ for FTY720-P. For calculation an external standard method using a not weighted, linear regression for FTY720 and polynomial, 1/x weighted regression for FTY720-P was used. The parameters of the methods are summarized in Table S2.

### 2.8. Amyloid-β immunoassay

Proteins were extracted from the cortex as previously described [34] in three fractions: Tris buffer saline (TBS), TBS buffer containing 1% Triton-X 100 (TBST), and 70% formic acid (FA). Then, Aβ content was determined by enzyme-linked immunoassay (ELISA) [34,43]. Briefly, pre-coated the 96 well plate with 1 ug/mL 3D6 antibody [34] overnight, plates were washed and blocked with 4% not-fat milk blocking buffer. Next, a standard or homogenate samples were added to the wells for 1 h. The biotinylated 20C2 antibody[34] was used for detection. The absorbance was measured at 450 nm with PerkinElmer 2030 manager system.

### 2.9. Reverse transcription polymerase chain reaction (RT-PCR)

Total RNA was isolated from 20 to 50 mg of the cortex using Trizol

reagent (Invitrogen). One microgram of total RNA was treated with DNAse I and transcribed into cDNA (Superscript III, Invitrogen). qPCR was performed in duplicate with SensiMix™ SYBR® Low-ROX Kit (Bioline) using the set of primers reported in Table S3. Fold changes of expression relative to control were determined after normalization to HRPT. Fold change was calculated by the comparative Ct method.

### 2.10. Statistics

Outcome parameters were analyzed with IBM SPSS Statistics for Windows version 27.0 with a two-way ANOVA with genotype and treatment as independent factors, and post hoc analysis was followed with Fisher's least significant difference (LSD) or Tukey HSD test. Extreme values identified in the sphingolipid analysis by the Dixon-test ($\alpha = 0.05$) were excluded from the dataset [44]. Using Dixon-test, we excluded a total of 2 animals belonging to the APOE4 and E4FAD group in the data set reported in Fig. 1 C and D. To evaluate if specific experimental groups performed above chance level, a one-sided t-test (if normally distributed) or Wilcoxon signed rank test was applied. Latency outcome was also analyzed by Cox regression modeling to cope with animals that failed to escape during the given time for the trials (60 s) [45]. Lipidomic data are reported as a volcano plot with $Log_{10}$ cut off of 1.3. Logistic regression was performed with SPSS. All graphs were designed with GraphPad Prism version 8.4.3 (686). A *F*-test or *p*-value of $< 0.05$ was considered significant.

### 2.11. Study approval

All animal experiments were approved by the Animal Welfare Committee of Maastricht University and followed the laws, rules, and guidelines of the Netherlands.

## 3. Results

### 3.1. The levels of Cer d18:1/16:0 and Cer d18:1/22:0 are increased in FAD

The impact of APOE3 and APOE4 on sphingolipid levels in the AD brain is understudied. Additionally, it is unknown if S1P production is reduced in FAD mice, modeling the observation made in AD patients [12]. Therefore, we investigated sphingolipid levels by mass spectrometry in the cortex of APOE3, APOE4 (Control) and E3FAD, E4FAD (FAD). The Cers, dihydroceramides, SMs, sterols (CE), and monohexyl-ceramides (Hex) expressed as a percentage of the class were mildly affected by the FAD genes (Fig. 1 A). CE (18:1) was found elevated while HexCer d18:1/20:2 and the Cer d18:1/18:3 were downregulated. The APOE4 background had a strong impact on SMs. SM d18:1/22:1, SM d18:1/14:1 and SM d18:1/18:3 were found significantly increased while SM d18:1/18:0 and SM d18:1/26:0 were reduced in APOE4 as compared to APOE3 mice (Fig. 1B). Relative quantification of Cer and SM species depicted a significant increase of Cer d18:1/16:0 (F

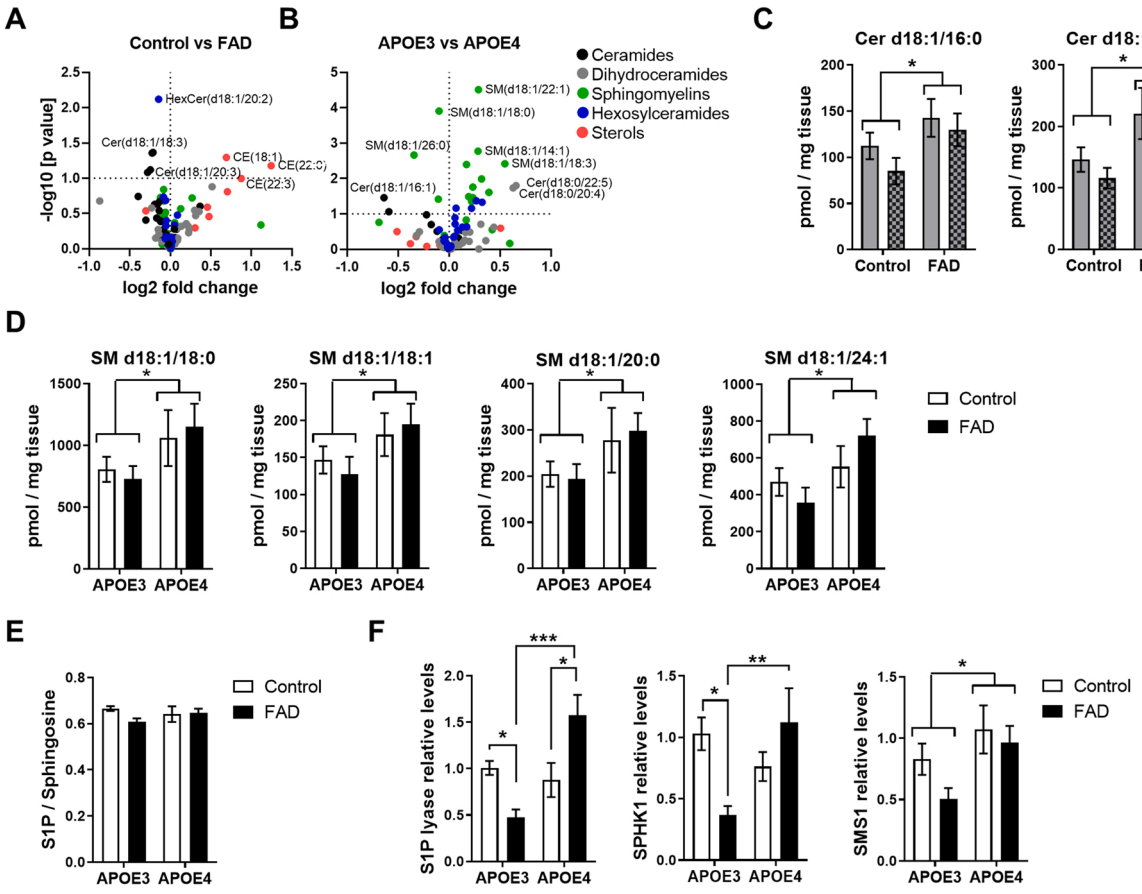


**Fig. 1.** S1P production and degradation are altered in FAD mice. A-B) Volcano plots of ceramides, dihydroceramide sphingomyelins hexosyl-ceramides and sterols measurements in the cortex depicting the difference between control (APOE3 N = 5 and APOE4 N = 5) versus FAD (E3FAD N = 5 and E4FAD N = 5) or APOE3 (APOE3 N = 5 and E3FAD N = 5) versus APOE4 (APOE4 N = 5 and E4FAD N = 5). C) Bars represent the mean ± S.E.M of Cer d18:1/16:0, Cer d18:1/22:0 and D) SM d18:1/18:0, SM d18:1/18:1, SM d18:1/20:0 and SM d18:1/24:1 measured in the cortex. Sphingolipid levels are expressed as pmol/mg tissue with N = 8–11 / group (two-way ANOVA, F test, *p < 0.05). E) Bar graph represents the mean ± S.E.M of the ratio S1P / sphingosine measured in the cortex of APOE3 (N = 5), APOE4 (N = 5), E3FAD (N = 5) and E4FAD (N = 5). F) Bar graph represents fold change of mRNA levels of S1P lyase, SPHK1 and SMS1 in the cortex of APOE3 (N = 4), APOE4 (N = 4), E3FAD (N = 5) and E4FAD (N = 5). Two-way ANOVA, LSD post-hoc, *p < 0.05, **p < 0.01 and ***p < 0.001.

(1, 35)= 4.73, p = 0.0363, ANOVA) and Cer d18:1/22:0 (F(1, 34) = 6.36, p = 0.0165, ANOVA) in the cortex of FAD mice, which was independent of APOE genetic background (Fig. 1 C). The SM species were increased in the APOE4 carriers: SM d18:1/18:0 (F(1, 35)= 4.51, p = 0.0408, ANOVA), SM d18:1/18:1 (F(1, 35)= 4.14, p = 0.0495, ANOVA), SM d18:1/20:0 (F(1, 36)= 4.11, p = 0.0500, ANOVA) and SM d18:1/24:1 (F(1, 35)= 6.21, p = 0.0175, ANOVA) (Fig. 1D). The ratio of S1P/sphingosine was similar in all genotypes (Fig. 1E). The S1P/sphingosine mean of E3FAD was lower than APOE3, but this tendency was not significant upon multiple test correction (uncorrected p value = 0.0138). However, expression levels of S1P lyase, which degrades S1P, was higher in E4FAD (interaction APOE-FAD, F(1, 14)= 14.81, p = 0.0018, and APOE main effect F(1, 14)= 9.18, p = 0.0090, ANOVA), while SPHK1, which produces S1P, was reduced in E3FAD mice (interaction APOE-FAD, F(1, 14)= 7.934, p = 0.0137, ANOVA) (Fig. 1 F). Also, SM synthase 1 (SMS1) expression was particularly high in APOE4 carriers (main effect APOE, F(1, 15)= 5.86, p = 0.0286, ANOVA) (Fig. 1 F). Our data indicate that certain Cer species, like Cer d18:1/16:0 and Cer d18:1/22:0 are increased in FAD transgenic mice and that the genes controlling S1P breakdown or production are altered in FAD depending on APOE genotype.

### 3.2. APOE4 genotype is associated with high levels of Cer d18:1/20:0 and Cer d18:1/22:0 in plasma and S1P plasma levels predict memory performance in WM

High levels of blood circulating Cer have been associated with an increased risk of developing memory impairment in a cohort of females [46,47]. Here, we analyzed Cer, S1P and SM levels at 10, 16, 20 and 28 weeks of age in the four genotypes. At week 28, Cer d18:1/20:0 (F(1, 108)= 14.54, p = 0.0007, ANOVA) and Cer d18:1/22:0 (F(1, 108)= 14.32, p = 0.0007, ANOVA) levels were increased in APOE4 carriers compared to APOE3 mice. Meanwhile Cer d18:1/24:0 (F(1, 108)= 8.03, p = 0.0085, ANOVA) and Cer d18:1/24:1 (FAD main effect F(1, 108)= 5.02, p = 0.0334; APOE main effect F(1, 108)= 6.03, p = 0.0207, ANOVA) were reduced at week 20 (Fig. 2 A). Furthermore, the specie Cer d18:1/24:1 was reduced in APOE4 compared to APOE3 and FAD mice compared to control at week 16 (Fig. 2 A). Plasma levels of SM d18:1/18:0 (F(1, 108)= 6.04, p = 0.0206, ANOVA) and SM d18:1/22:0 (F(1, 108)= 5.11, p = 0.0320; F(1, 108)= 13.22, p = 0.0011, ANOVA) were elevated in APOE4 carriers at 10 or 16 and 28 weeks of age, respectively (Fig. 2B). Interestingly, S1P levels were low at 16 weeks of age in FAD (F(1, 35)= 4.22, p = 0.0474, ANOVA) and APOE4 carriers (F (1, 35) = 22.45, p < 0.0001, ANOVA) (Fig. 2 C). Reduction of S1P at week 10 (unpaired t-test, p = 0.0018) and 16 (unpaired t-test, p = 0.0133) was associated with an increased likelihood of failing the WM test (Fig. 2D). Therefore, logistic regression was performed to verify

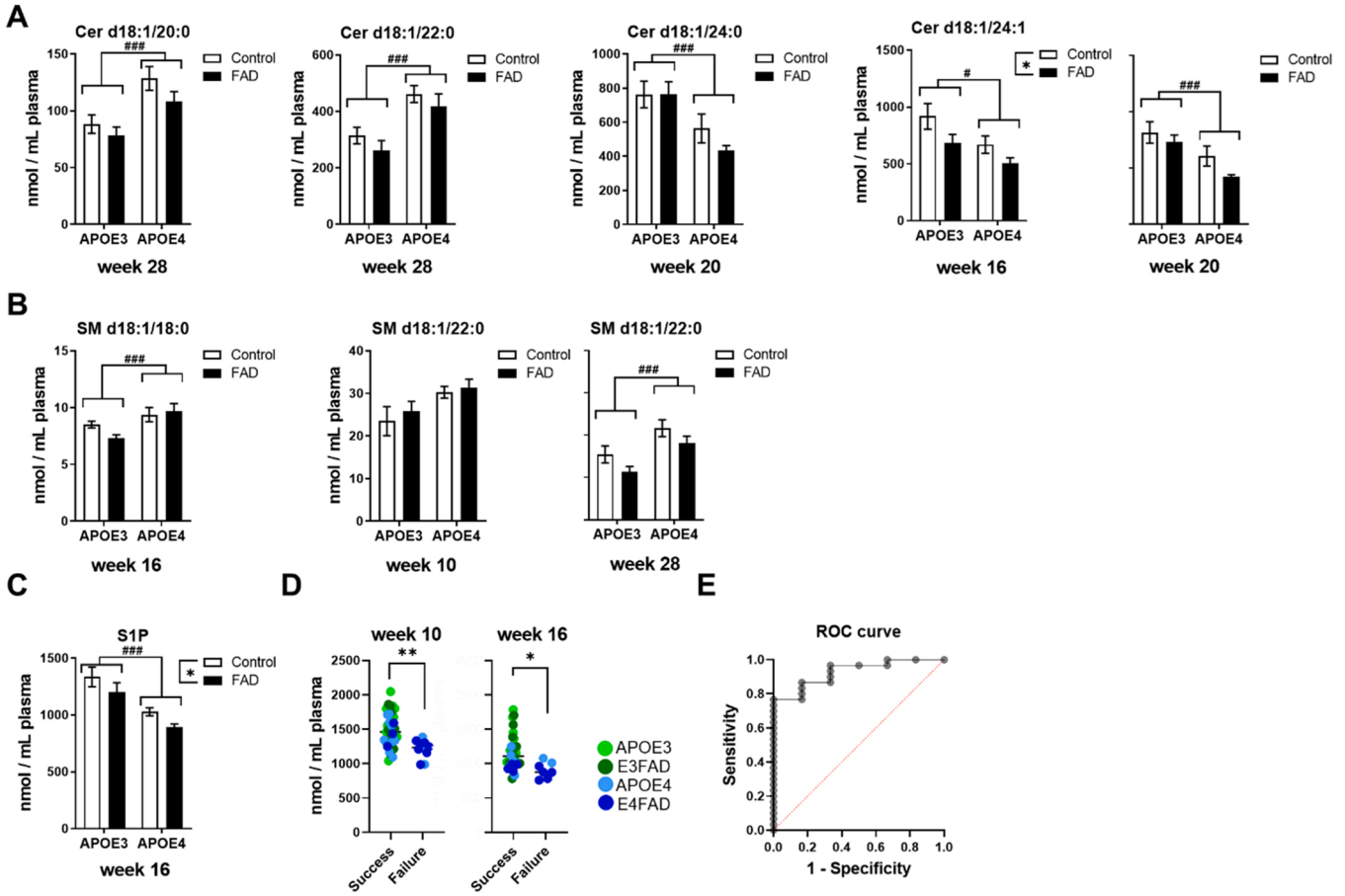


**Fig. 2.** APOE4 carriers are characterized by high levels of Cer d18:1/18:0 and SM d18:1/20:0 in plasma and S1P plasma levels predict memory performance in WM. A) Cer and B) SM were measured in plasma at 10, 16, 20, and 28 weeks of age by HPLC-MS/MS. Sphingolipid levels were expressed as pmol/μL plasma. Bars represent the mean ± S.E.M per group N = 6–9 (Two-Way Repeated Measures ANOVA, APOE main effect $^{\#}p < 0.05$; $^{\#\#}p < 0.01$, main effect of FAD *p < 0.05). C) S1P levels were measured in plasma at 16 weeks by HPLC-MS/MS. (Two-Way ANOVA, APOE main effect ###p < 0.01, main effect of FAD *p < 0.05). D) Scatter plot of S1P levels measured at weeks 10 and 16 of age in the group that had success or failed the WM test. (Unpaired t-test, *p < 0.05, **p < 0.01). E) ROC curve of logistic regression of S1P levels and WM maze success plotted with the true positive rate (Sensitivity) in the function of the false positive rate (1-Specificity) for different cut-off points.

if S1P levels could predict the failure to find the platform during the probe trial of the WM. The logistic regression model was statistically significant, $\chi 2(4) = 18.672$, $p < 0.001$. The model explained 72.3% (Nagelkerke R2) of the variance in WM test and correctly classified 96.8% of mice who failed the test (Fig. 2E). Our data indicates Cer d18:1/20:0 and Cer d18:1/22:0, and SM d18:1/22:0 are increased in APOE4 at week 28 of age. Furthermore, low levels of S1P in the plasma, at week 10 and 16 especially, is associated with an increased likelihood of failing WM probe test.

### 3.3. APOE4 genes reduce blood circulating leukocytes

Women carrying the APOE4 gene showed an early reduction of the circulating white blood cells CD4 + Th cells, which are important in the adaptive immune response to Aβ [48]. This observation prompted us to study the white cell composition in the blood of the APOE4 female mice. FAC analysis of blood samples collected at 28 weeks of age indicated that females who carry APOE4 had not only a reduced number of CD4 + Th cells but also reduced counts of b220 + B cells ($F(2, 34) = 14.80$, $p < 0.0001$, ANOVA), neutrophils ($F(1, 11) = 13.64$, $p = 0.0035$, ANOVA), eosinophils ($F(1, 11) = 5.77$, $p = 0.0351$, ANOVA), CD8 +T cytotoxic cells ($F(1, 11) = 8.14$, $p = 0.0157$, ANOVA) and CD3 +T cells ($F(1, 11) = 6.44$, $p = 0.0276$, ANOVA) (Fig. 3).

### 3.4. FTY720 prevents memory impairments in E4FAD mice and anxious behavior in APOE4 mice

During FTY720 administration, animal welfare was assessed daily by expert personnel and no abnormalities were found on social behavior, nesting, grooming, pain behavior and animal activity. Furthermore, a significant increase of weight in time was observed in all groups suggesting that mice well tolerated both doses for about 15 weeks (Fig. 4 A). FTY720 and the phosphorylated form (FTY720-P) were measured in blood and brain tissue to ensure the correct dosing of the drug (Fig. 4B). On average, 68% of the blood circulating FTY720 was phosphorylated, while in the brain the 88% was (Fig. 4B). In the WM, E4FAD mice had

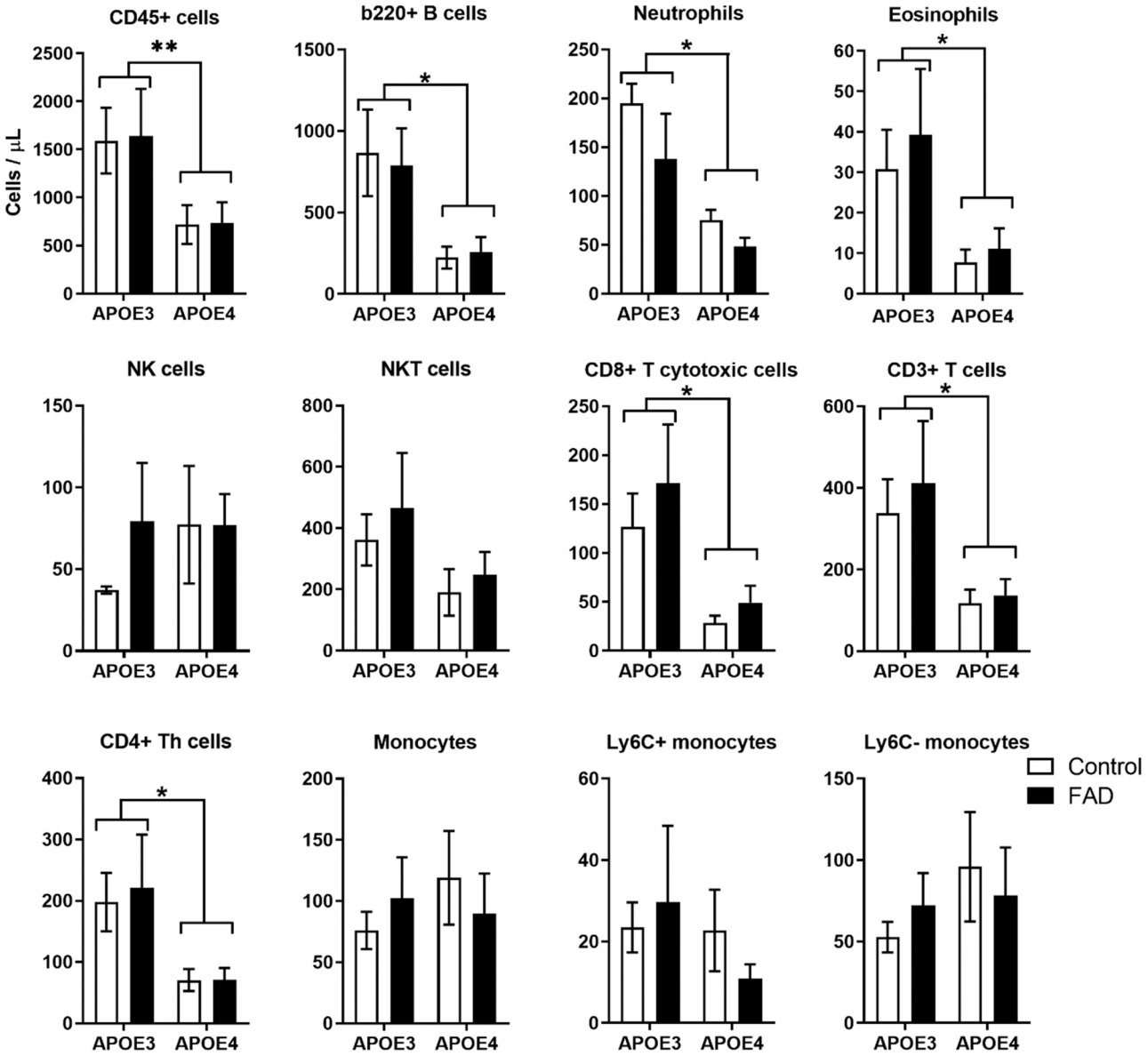


**Fig. 3.** White blood cells profile in APOE3, E3FAD, APOE4 and E4FAD mice at 28 weeks of age. White blood cells analyzed by FACS in blood samples collected at week 26–28 of animal age were sorted between: CD45 + b220 +B, neutrophil, eosinophil, NK cells, CD8 +T cytotoxic, CD3 +T, monocytes, Ly6C+ and Ly6C-. Each bar represents the mean + /-SEM of 4 animals / group (ANOVA, APOE main effect; *$p < 0.05$).

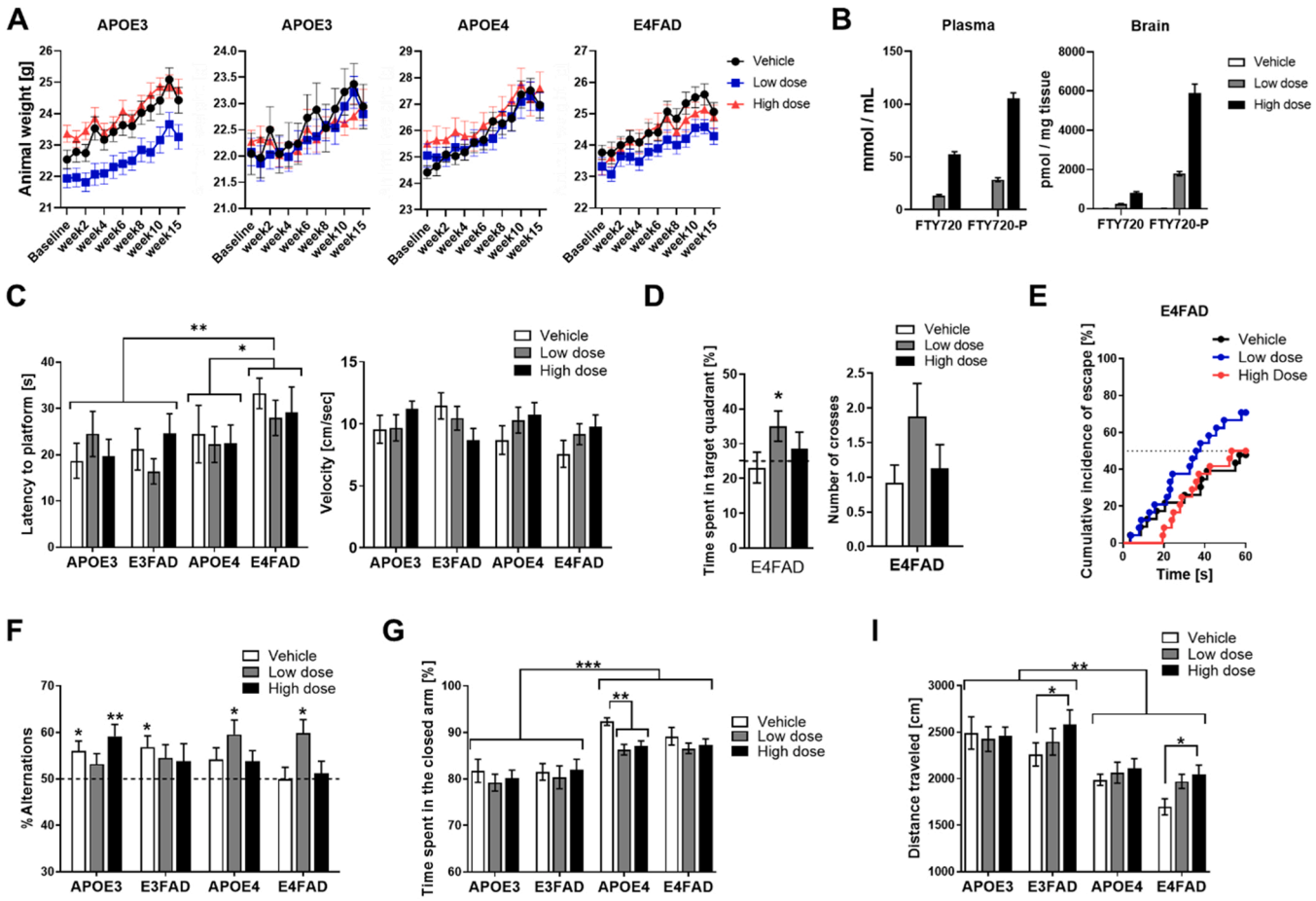


**Fig. 4.** FTY720 prevents memory impairments in E4FAD mice and anxious behavior in APOE4 mice. A) Animal weight measured during the experiment grouped based on treatment for each genotype (APOE3, E3FAD, APOE4 and E4FAD). Each bar represents the mean + /-SEM of 21–25 animals. B) Plasma and brain FTY720 concentrations of unphosphorylated (FTY720) and phosphorylated (FTY720-P) at the end of experiment (Vehicle N = 24, Low dose (0.1 mg / kg) N = 24, High dose (0.5 mg / kg) N = 24). C) The average of latency expressed in seconds (s) measured during the probe trial and the average velocity of each experimental group. Each bar represents the mean + /-SEM of 21–25 animals (ANOVA, LSD post hoc, *p < 0.05; ** p < 0.01). D) The percentage of time spent in the target quadrant compared to chance level 25% and number of crosses of E4FAD groups (one sample t-test *p < 0.05). E) Cumulative incidence plots of spatial memory retention data of E4FAD groups. F) The percentages of correct alternations were measured over 10 triads. The percentage of each group was then compared to the 50% chance levels (one sample t test * p < 0.05). Each bar represents the mean + /-SEM of 21–25 animals. G) Anxiety is expressed as percentages of time spent in the close arms. Each bar represents the mean + /-SEM of 21–25 animals, (ANOVA, Tukey post-hoc, ** p < 0.01, ***p < 0.001). I) Distance traveled in the OF test in the vehicle and drug-treated groups of APOE3, E3FAD, APOE4, and E4FAD animals. Each bar represents the mean + /-SEM of 4 animals (ANOVA, Tukey post-hoc * p < 0.05, ** p < 0.01).

the worst scores in the test (genotype main effect, $F$ (3, 161)= 3.04, $p$ = 0.0306, ANOVA, APOE3 vs E4FAD p = 0.0089, E3FAD vs E4FAD p = 0.0092, APOE4 vs E4FAD p = 0.0497) even though all groups had similar velocities (Fig. 4 C). E3FAD mice did not show a significant memory impairment compared to their litter controls APOE3 mice (Fig. 4 C). Next, we analyzed the FTY720 dose-response in the E4FAD mice, which manifested the memory impairment. The low dose increased the time spent in the target quadrant (one sample t-test, p = 0.0392) (Fig. 4D). Also, the number of times the mice crossed the platform area was 1.9x (STDEV +/−2.3) higher in the low dose group of E4FAD compared to vehicle (Fig. 4D). When data was analyzed using cox regression analysis, following Jahn-Eimernacher et al., an alternative approach for statistical analyses of latency outcome [45], we found that the low dose increased by 1.8-fold the number of mice that found the platform in E4FAD groups (HR=1.821 95%-CI 0.869–3.816) (Fig. 4E). The AYM was performed as a second memory paradigm. The test did not detect the genotype difference with the sensitivity of the WM (Fig. 4F). However, the low dose significantly increased the percentage of correct triades in the APOE4 and E4FAD genotypes, when considering the initial 10 alternations (Fig. 4F). The cumulative alternation of the complete trials for all experimental group is reported in (Figure S2A). In the EZM, APOE4 carriers were characterized by increased anxiety (APOE main effect, F(3, 267)= 17.97, p < 0.0001, ANOVA) and FTY720 reduced anxiety in the APOE4 mice independently from dose (treatment main effect, F(2, 267)= 3.21, p = 0.0417, ANOVA, APOE4:Vehicle vs APOE4:Low dose p = 0.0163, APOE4:Vehicle vs APOE4:High dose, p = 0.0329) (Fig. 4 G). This drug effect was not correlated to mobility differences during the trial (Figure S2B). When analyzing distance traveled in the OF over 20 min trials, we found a strong genotype effect due to APOE background. The APOE4 carriers traveled significantly less than the APOE3 carriers (APOE main effect, F(3, 267) = 15.82, p < 0.0001, ANOVA) (Fig. 4I). E3FAD and E4FAD treated with the high dose traveled longer distances than the control groups (treatment main effect F(2, 267)= 3.21, p = 0.0417, ANOVA) (Fig. 4I), suggesting that the drug affects mobility. Our data indicate that FTY720 prevented E4FAD memory impairment in two memory paradigms and reduced anxious behavior in APOE4. Also, the high dose increases the mobility of the E3FAD and E4FAD in the locomotion test.

### 3.5. FTY720 reduces circulating leukocytes, neuroinflammation and Aβ levels in the FA fraction of E4FAD

FTY720 is known to reduce leukocyte migration to the CNS by diminishing the numbers of circulating leukocytes. Therefore, we measured peripheral white blood cells by flow cytometry at the end of the experiment. We found that both treatment regimens decreased the number of CD45 + cells($F(2, 16)= 7.14$, $p = 0.0061$, ANOVA), b220 +B cells ($F(2, 16)= 11.50$, $p = 0.0008$, ANOVA), NKT ($F(2, 16)= 7.62$, $p = 0.0047$, ANOVA), CD8 +T cytotoxic cells ($F(2, 16)= 9.66$, $p = 0.0018$, ANOVA), CD3 +T ($F(1, 11)= 6.44$, $p = 0.0276$, ANOVA) and CD4 +Th cells ($F(2, 16)= 7.85$, $p = 0.0042$, ANOVA), while neutrophils, eosinophils, NK cells, monocytes, Ly6C+ and Ly6C- monocytes remained unchanged (Fig. 5 A). In the brain, FTY720 reduced expression levels of CD86, a marker for microglia pro-inflammatory status (genotype main effect $F(1, 23)= 9.14$, $p = 0.0060$, interaction APOE-treatment, $F(2, 23)= 4.91$, $p = 0.0167$, ANOVA) (Fig. 5B). When quantifying Aβ in the cortex of E3FAD and E4FAD by ELISA, we found that Aβ levels were higher in E4FAD compared to E3FAD mice ($F(1, 48)= 23.32$, $p < 0.0001$, ANOVA), and FTY720 reduced the concentration of Aβ in the FA fraction to 51.9% in E4FAD ($F(2, 38)= 3.37$, $p = 0.0448$, ANOVA) (Fig. 5C).

### 3.6. FTY720 decreases Cer and SM in the cortex of FAD mice

Sphingolipid analysis of the cortex revealed that FTY720 high dose, especially, decreased Cer d18:1/14:0 ($F(2, 52)= 5.93$, $p = 0.0048$, ANOVA), Cer d18:1/16:0 ($F(2, 52)= 6.51$, $p = 0.0030$, ANOVA) and Cer d18:1/18:0 levels ($F(2, 52)= 4.12$, $p = 0.0218$, ANOVA) in E4FAD. In the E3FAD, the high dose of FTY720 reduced Cer d18:1/16:0 ($F(2, 52)= 6.51$, $p = 0.0030$, ANOVA), Cer d18:1/18:0 ($F(2, 52)= 4.12$, $p = 0.0218$, ANOVA), Cer d18:1/20:0 ($F(2, 52)= 4.19$, $p = 0.0205$, ANOVA), Cer d18:1/22:0 ($F(2, 52)= 4.09$, $p = 0.0223$, ANOVA) and Cer d18:1/24:1 levels ($F(2, 51)= 3.51$, $p = 0.0372$, ANOVA) (Fig. 6 A). Surprisingly, SM d18:1/18:0 (interaction APOE-treatment $F(2, 52)= 5.75$, $p = 0.0055$), SM d18:1/18:1 (interaction APOE-treatment $F(2, 53)= 5.37$, $p = 0.0075$), SM d18:1/20:0 (interaction APOE-treatment $F(2, 52)= 5.38$, $p = 0.0075$) and SM d18:1/24:1 concentration (interaction APOE-treatment $F(2, 52)= 3.70$, $p = 0.0312$) were lower only in E4FAD groups treated with FTY720, particularly low dose (Fig. 6B). Quantification of Cer, dihydroCer, SMs, sterols and monohexyl-Cer as percentage of the class in E4FAD, showed similar pattern, where low dose affected especially SM, overall (Fig. 6C).

## 4. Discussion

The neuroprotection mediated by S1P signaling declines during the course of AD pathogenesis, especially in APOE4 carriers [12]. Therefore, in this work, we investigated the pharmacology of the S1P mimicking drug FTY720 in preventing memory impairment in a mouse model of FAD carrying APOE4 genes. Drug effects on blood circulating sphingolipids were monitored during FTY720 administration, which lasted for

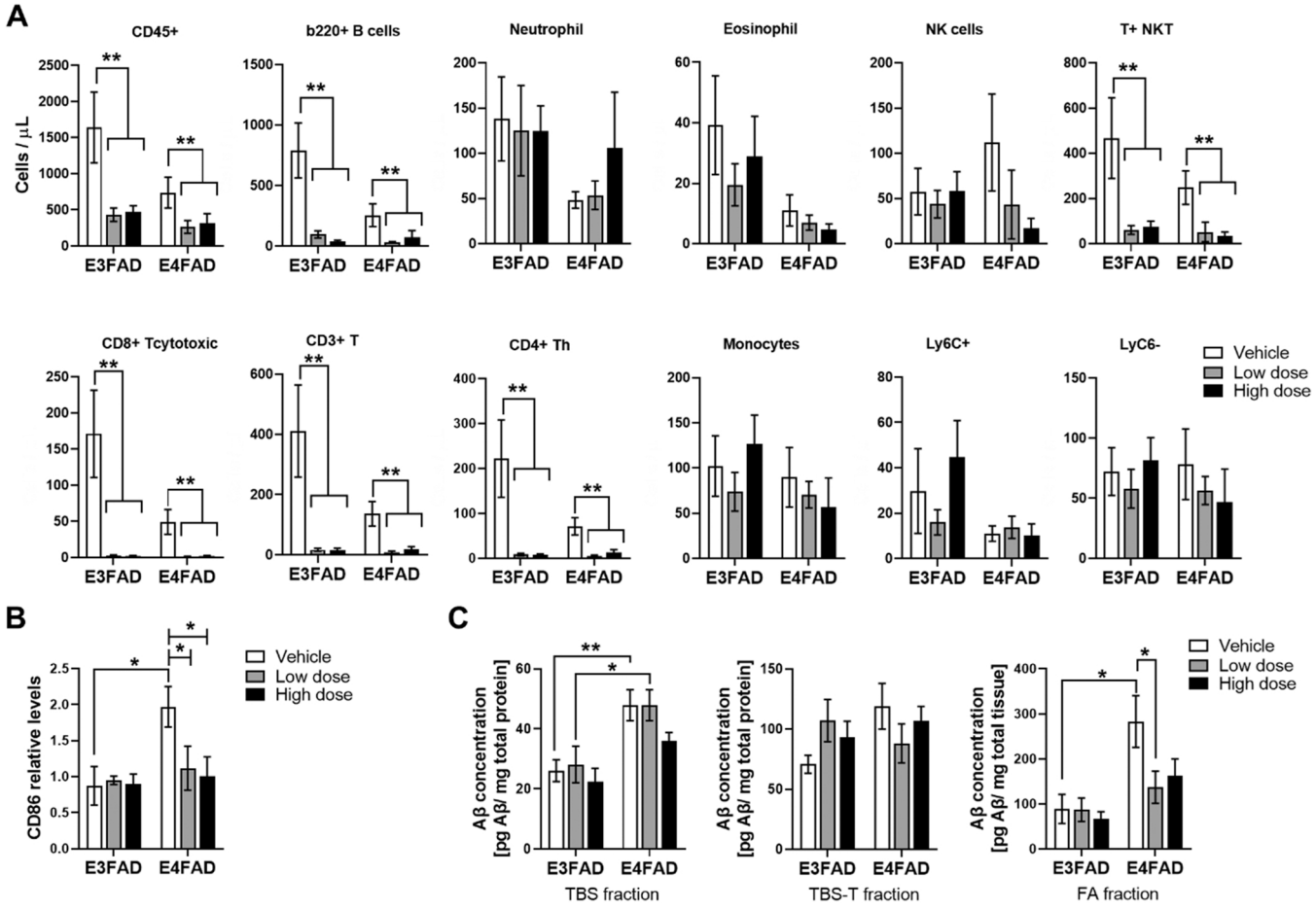


**Fig. 5.** FTY720 reduces circulating leukocytes, neuroinflammation and Aβ levels in the FA fraction of E4FAD. A) FACS analysis of the following white blood cells: CD45 + b220 +B, neutrophil, eosinophil, NK cells, NKT, CD8 +T cytotoxic, CD3 +T, CD4 +Th, monocytes, Ly6C+ and Ly6C-. Each bar represents the mean + /-SEM of 3–4 animals/group (ANOVA, Tukey post hoc; **$p < 0.01$). B) Expression levels of CD86 in the cortex. Each bar represents the mean + /-SEM of 4–5 animals/group (ANOVA, Tukey post hoc; *$p < 0.05$). C) Aβ quantification in three extraction buffers, TBS, TBS-T, and formic acid (FA) by ELISA in the cortex of E4FAD mice compared to E3FAD animals. Each bar represents the mean + /-SEM of 6–9 animals, ANOVA, Tukey post hoc, *$p < 0.05$; * *$p < 0.01$).

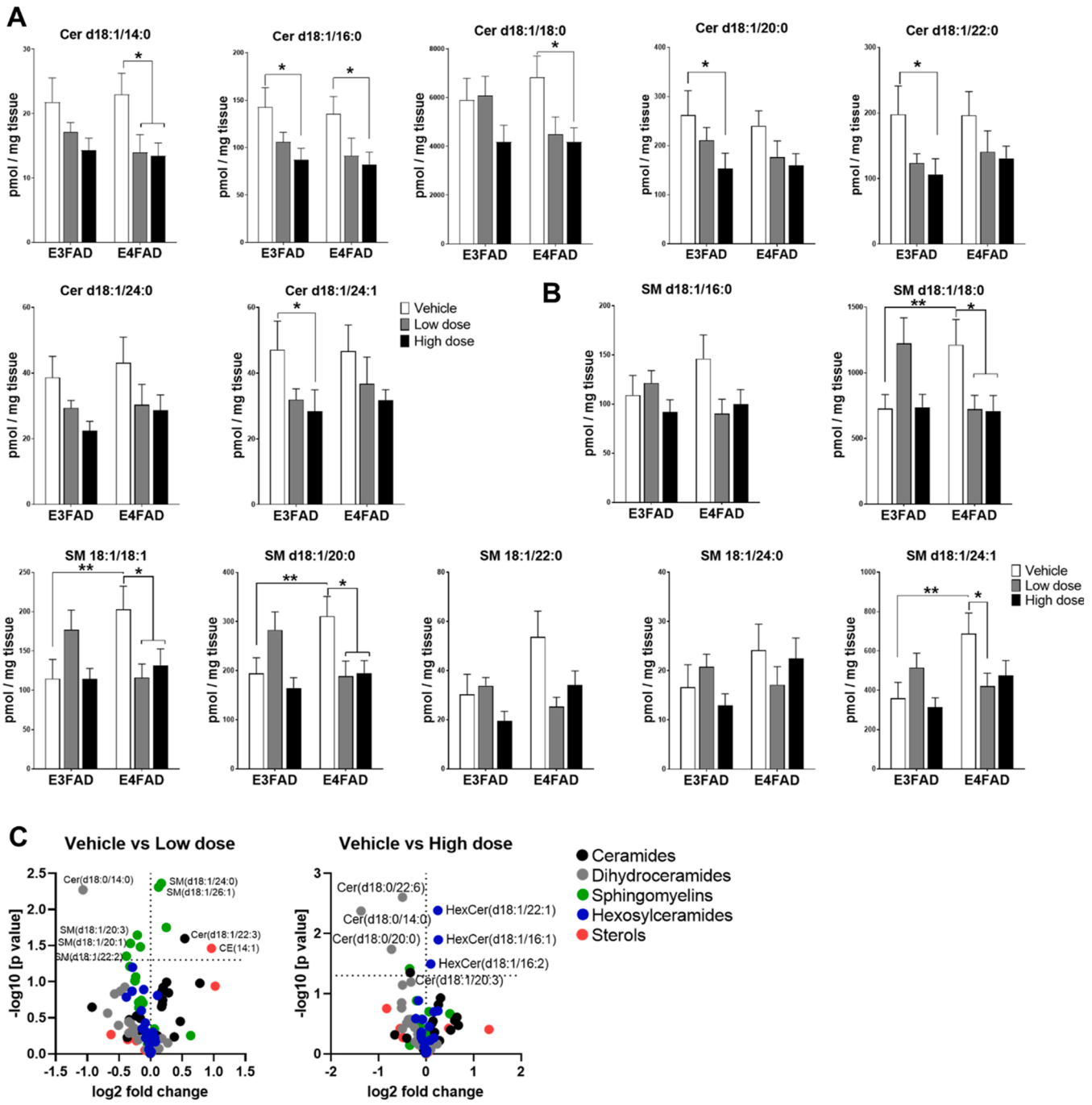


**Fig. 6.** FTY720 reduces Cer and SM in the cortex of FAD mice. A) Bars represent the mean ± S.E.M of Cer d18:1/14:0, Cer d18:1/16:0, Cer d18:1/18:0, Cer d18:1/20:0, Cer d18:1/22:0, Cer d18:1/24:0, Cer d18:1/24:1, and B) SM d18:1/16:0, SM d18:1/18:0, SM d18:1/18:1, SM d18:1/20:0 SM d18:1/22:0, SM d18:1/24:0,and SM d18:1/24:1 measured in the cortex. Sphingolipid levels are expressed as pmol/mg tissue with N = 9–10 / group (ANOVA, LSD post-hoc, *$p < 0.05$, **$p < 0.01$). C) Volcano plots of Cers, dihydroceramide SMs hexosyl-ceramides and sterols measurements in the cortex depicting difference between vehicle versus FTY720 low or high dose in E4FAD (Vehicle N = 5, Low dose N = 5, and High dose N = 5).

15 weeks. Furthermore, we studied the effect of FTY720 on 124 sphingolipids and 22 sterols in the cortex by mass spectrometry. We discovered that enzymes responsible for S1P production or turn-over are altered in FAD mice. At 10–16 weeks of age, S1P levels in plasma predicted the mice's rate of success in the memory test. Administration of FTY720 prevented memory impairment in E4FAD and attenuated anxious behavior in APOE4 animals. Upon FTY720 treatment, blood circulating leukocytes were significantly decreased, and, in the cortex, the expression of pro-inflammation marker CD86 was downregulated. Sphingolipid analysis in the brain indicated a reduction of Cer and SM levels. Biochemical analysis of the cortex showed that FTY720 reduced insoluble Aβ concentration by about 51.9%.

Having one or two APOE4 alleles increases the risk factor of developing AD and is associated with earlier age of disease onset. Interestingly, Couttas et al., reported that S1P production in the brain is associated with APOE4 genes and is compromised early during AD process [12]. The ratio of S1P over sphingosine was reduced early in the CA1 of the hippocampus and in the middle temporal gyrus, particularly in APOE4 carriers. This was caused by a downregulation of SPHK1 and upregulation of S1P lyase [12]. Similarly, in our work, we found that

SPHK1 and S1P lyase expression are altered in the cortex of FAD mice. However, we did not find a significant difference in the ratio of S1P to sphingosine in FAD mice. This is in alignment with the observation made by Couttas et al., on $APP_{swe}/PS1_{\Delta E9}$ mice where Aβ overproduction did not cause a reduction in normalised S1P [12]. Notably, in the plasma we found that S1P was significantly reduced in FAD mice and in general in APOE4 carriers at 16 weeks of age. Having low levels of plasma S1P increased the chances of failing the WM test. The concept that plasma levels of S1P and its metabolites could be used to diagnose neurodegeneration is under investigation with promising results [49]. S1P ratio to short chain sphingosine (d16:1) seems to correlate with inflammation-associated neurodegeneration [49]. Furthermore, in females, which are more likely to develop AD, plasma levels of S1P decreases with aging and during menopause probably in response to estradiol fluctuation [50]. Here, we show that S1P plasma levels can provide early indication of cognitive decline, before any signs of memory impairments are evident.

APOE4 proteins can affect circulating leukocytes when there is an accumulation of APOE in the plasma [51]. Additionally, women carrying the APOE4 gene showed an early reduction of the circulating white blood cells CD4 + Th, which are important in the adaptive immune response to Aβ [48]. In this work, we also found that blood circulating white cells are highly affected by APOE4 genes. The number of circulating b220 + B cells, neutrophils, eosinophils, CD8 +T cytotoxic, CD3 +T and CD4 +Th cells were lower in APOE4 mice compared to APOE3. The cross talk between peripheral immunity and brain function seems to play a role in aging and AD [52,53]. The blood leukocytes decrease in the elderly as a process of aging [54]. Furthermore, CD4 + Th cells and neutrophils migrate and populate the meninges and choroid plexus building a direct interface with the brain parenchyma [55]. Activation of CD4 + Th cells cause secretion of the cytokines, IL-6 and IFNγ, which affects cognition in mice [52], while neutrophils, which have been detected in the brain of 5xFAD mice, were found to promote amyloid plaques [56]. Therefore, what we observed in APOE4 genotypes might be an accelerated process of aging impacting the peripheral immune system [52]. The significance of APOE4 effects on peripheral white blood cells, with the downstream effects on brain function, is yet to be understood.

APOE4 background had also a strong impact on mice behavior in locomotor and anxiety tasks especially. As previously reported, APOE4 transgenic mice were less active in the OF task [57] and displayed increased anxiety in the EZM [58]. The abnormalities in anxious behavior are thought to be caused by reduced ApoE expression in the amygdala, the brain center important for fear and anxiety processing [58]. In the memory test WM, the E4FAD was the only genotype showing memory impairments at 28 weeks of age. This was probably due to the more severe Aβ pathology that these transgenic mice display compared to E3FAD [59]. In the WM, the E4FAD FTY720 treated animals spent more time in the target quadrant and crossed the platform area 1.9 x more than the control mice. These observations in memory quality were confirmed by a second independent memory test: the AYM test. These findings are in alignment with previous observation on other AD induced-models where FTY720 improved memory in behavioral tests [28,29].

As previously reported, we found that in the cortex of the FAD mice the Cer d18:1/16:0 and Cer d18:1/22:0 levels were elevated [34], phenocopying brain of frontotemporal lobar dementia and AD patients [10,60]. Cer d18:1/16:0 and Cer d18:1/22:0 are mainly produced by Cer synthase 5 (CerS5) and 2 (CerS2), respectively [61,62]. CerS2 and CerS5 seem to drive Cer production in astrocytes during inflammation [63]. Astrocytic Cer is extremely toxic to neurons. When activated, astrocytes release extracellular vesicles highly enriched in Cer, which significantly enhance Aβ toxicity by attacking mitochondria in neurons [64].

The most prominent effects of FTY720 on cerebral sphingolipid levels were observed in the E4FAD mice. Most of the Cer species were downregulated upon FTY720 administration, including Cer d18:1/16:0 and Cer d18:1/22:0. The reduction of Cer species may be the result of the multi-target action of FTY720. Recently, new pharmacological mechanisms have been discovered for FTY720. Firstly, it was reported that FTY720 functionally inhibits acid sphingomyelinase (A-SMase) [65]. SMases are a family of phosphodiesterases, which preferentially hydrolyze SM, producing phosphorylcholine and Cer [66,67]. Secondly, it was found that FTY720 in human pulmonary artery endothelial cells can inhibit Cer synthase (CerS) decreasing Cer with IC50 of 6.4 + /− 1 μM [68]. The inhibitory action of FTY720 on CerS and A-SMase, two enzymes responsible of Cer synthesis, may explain the Cer reduction. Additionally, FTY720 has proven to control the transcription of genes belonging to the sphingolipid metabolism. Jęśko et al. reported that FTY720 downregulates CerS2, therefore, reducing production of long-chain Cer and upregulates neutral sphingomyelinase 2 (N-SMase-2) increasing SM breakdown [69]. These observations seemed to be dependent on age and AD [69]. The reported effect of FTY720 on CerS and N-SMase-2 mRNA levels may explain the reduction in Cer and SMs observed in the cortex of E4FAD. The low dose of FTY720 was more efficacious in coping with Aβ pathology in E4FAD. FTY720 reduced the concentration of Aβ concentration in FA fraction by about 51.9% in the cortex. Others have observed that Aβ plaques and neuroinflammation are more effectively countered using low doses of FTY720 [70]. According to in vitro studies FTY720 reduces Aβ release from neurons without activating downstream signaling pathways of S1P receptors [27]. Most interesting, it seems that the benefits of the drug on memory performance are independent of the effects on immune cells leading to peripheral lymphopenia [70]. This observation is extremely important when considering FTY720 for clinical trials. In fact, most of the side-effects of FTY720 observed during MS clinical trials could be alleviated when repurposing FTY720 for AD at a lower dose regimen. However, we cannot exclude that FTY720 beneficial effect is induced also by S1P receptors activation in brain cells. For instance S1P receptor deficiency in astrocytes protects from severe inflammation [71].

To conclude, we report that blood circulating S1P predicts memory decline in FAD mice models. Administration of FTY720 prevents memory impairment in E4FAD and attenuates anxious behavior in APOE4 animals. Furthermore, we validate secondary actions of FTY720 which are not mediated directly by S1P receptors, and shift the sphingolipid pathway towards Cer and SM reduction in the cortex. Our data confirms that targeting the sphingolipid metabolism might represent a valid system for developing new therapeutic drugs for AD.

## Data availability statement

The datasets used and/or analyzed during the current study are available from the corresponding author on reasonable request.

## CRediT authorship contribution statement

**Simone M. Crivelli**: Methodology, Formal analysis, Investigation, Data curation, Writing – original draft. **Mario Losen, Qian Luo, Daan van Kruining, Caterina Giovagnoni, Marina Mané-Damas, Sandra den Hoedt**: Methodology, Data curation, Writing – review & editing. **Dusan Berkes, Helga E. De Vries, Monique T. Mulder, Jochen Walter, Erhard Bieberich**: Conceptualization, Resources, Writing – review & editing, Funding acquisition. **Etienne Waelkens, Rita Derua, Johannes V. Swinnen, Jonas Dehairs, Erwin P.M. Wijnands**: Methodology, Writing – review & editing. **Pilar Martinez-Martinez**: Conceptualization, Resources, Methodology, Writing – review & editing, Supervision, Project administration, Funding acquisition.

## Permission to reproduce material from other sources

n/a.

## Conflict of interest statement

The authors declare no competing financial interests,

## Acknowledgments

This work was supported by grants to MTM, JW, AR, PMM, and HEV from the ZonMw Memorabel Program (project nr: 733050105), the Alzheimer Nederland (projectnr: 14545, The Netherlands) to PMM, the Interreg VA EMR program (EURLIPIDS, EMR23, The Netherlands) to EW and PM. Aspects of this work were supported by grants to QL (the China Scholarship Council 201706220095, China), EB (National Institutes of Health: R01AG034389, R01NS095215, R01AG064234; U.S. Department of Veterans Affairs: I01BX003643, USA) and to SMC (BrightFocus Grant Submission Number: A20201464F; National Institute On Aging of the National Institutes of Health under Award Number P30AG028383, USA). Acknowledgment is made to the donors of ADR, a program of BrightFocus Foundation. We acknowledge Christian Beerli for analyzing FTY720/-P levels and to Novartis Pharma AG for supplying the FTY720.

## Appendix A. Supporting information

Supplementary data associated with this article can be found in the online version at doi:10.1016/j.biopha.2022.113240.

## References

[1] J. Rogers, J.H. Morrison, Quantitative morphology and regional and laminar distributions of senile plaques in Alzheimer's disease, J. Neurosci. 5 (10) (1985) 2801–2808.
[2] H. Kawasaki, et al., Neurofibrillary tangles in human upper cervical ganglia. Morphological study with immunohistochemistry and electron microscopy, Acta Neuropathol. 75 (2) (1987) 156–159.
[3] H.M. Wisniewski, P.B. Kozlowski, Evidence for blood-brain barrier changes in senile dementia of the Alzheimer type (SDAT), Ann. N. Y Acad. Sci. 396 (1982) 119–129.
[4] D.J. Selkoe, Alzheimer's disease: genes, proteins, and therapy, Physiol. Rev. 81 (2) (2001) 741–766.
[5] S.M. Crivelli, et al., Sphingolipids in Alzheimer's disease, how can we target them? Adv. Drug Deliv. Rev. (2020).
[6] K. Czubowicz, R. Strosznajder, Ceramide in the molecular mechanisms of neuronal cell death. The role of sphingosine-1-phosphate, Mol. Neurobiol. 50 (1) (2014) 26–37.
[7] K. Yuyama, S. Mitsutake, Y. Igarashi, Pathological roles of ceramide and its metabolites in metabolic syndrome and Alzheimer's disease, Biochim Biophys. Acta 1841 (5) (2014) 793–798.
[8] N.M. de Wit, et al., Altered Sphingolipid balance in capillary cerebral amyloid angiopathy, J. Alzheimers Dis. 60 (3) (2017) 795–807.
[9] P. Katsel, C. Li, V. Haroutunian, Gene expression alterations in the sphingolipid metabolism pathways during progression of dementia and Alzheimer's disease: a shift toward ceramide accumulation at the earliest recognizable stages of Alzheimer's disease? Neurochem Res 32 (4–5) (2007) 845–856.
[10] R.G. Cutler, et al., Involvement of oxidative stress-induced abnormalities in ceramide and cholesterol metabolism in brain aging and Alzheimer's disease, Proc. Natl. Acad. Sci. USA 101 (7) (2004) 2070–2075.
[11] X. He, et al., Deregulation of sphingolipid metabolism in Alzheimer's disease, Neurobiol. Aging 31 (3) (2010) 398–408.
[12] T.A. Couttas, et al., Loss of the neuroprotective factor Sphingosine 1-phosphate early in Alzheimer's disease pathogenesis, Acta Neuropathol. Commun. 2 (2014) 9.
[13] J. Ceccom, et al., Reduced sphingosine kinase-1 and enhanced sphingosine 1-phosphate lyase expression demonstrate deregulated sphingosine 1-phosphate signaling in Alzheimer's disease, Acta Neuropathol. Commun. 2 (2014) 12.
[14] S.S. Chakrabarti, et al., Ceramide and sphingosine-1-phosphate in cell death pathways: relevance to the pathogenesis of Alzheimer's disease, Curr. Alzheimer Res 13 (11) (2016) 1232–1248.
[15] C. Malaplate-Armand, et al., Soluble oligomers of amyloid-beta peptide induce neuronal apoptosis by activating a cPLA2-dependent sphingomyelinase-ceramide pathway, Neurobiol. Dis. 23 (1) (2006) 178–189.
[16] A. Elsherbini, E. Bieberich, Ceramide and exosomes: a novel target in cancer biology and therapy, Adv. Cancer Res 140 (2018) 121–154.
[17] B. Kwon, et al., Synergistic effects of beta-amyloid and ceramide-induced insulin resistance on mitochondrial metabolism in neuronal cells, Biochim Biophys. Acta 1852 (9) (2015) 1810–1823.
[18] L. Puglielli, et al., Ceramide stabilizes beta-site amyloid precursor protein-cleaving enzyme 1 and promotes amyloid beta-peptide biogenesis, J. Biol. Chem. 278 (22) (2003) 19777–19783.
[19] N. Takasugi, et al., Synthetic ceramide analogues increase amyloid-beta 42 production by modulating gamma-secretase activity, Biochem Biophys. Res Commun. 457 (2) (2015) 194–199.
[20] I.Y. Tamboli, et al., Sphingolipid storage affects autophagic metabolism of the amyloid precursor protein and promotes Abeta generation, J. Neurosci. 31 (5) (2011) 1837–1849.
[21] K. Matsuzaki, K. Kato, K. Yanagisawa, Ganglioside-mediated assembly of amyloid β-protein: roles in Alzheimer's disease, Prog. Mol. Biol. Transl. Sci. 156 (2018) 413–434.
[22] M.O. Grimm, et al., APP function and lipids: a bidirectional link, Front Mol. Neurosci. 10 (2017) 63.
[23] G. Wang, et al., Astrocytes secrete exosomes enriched with proapoptotic ceramide and prostate apoptosis response 4 (PAR-4): potential mechanism of apoptosis induction in Alzheimer disease (AD), J. Biol. Chem. 287 (25) (2012), 21384-95.
[24] V. Brinkmann, et al., Fingolimod (FTY720): discovery and development of an oral drug to treat multiple sclerosis, Nat. Rev. Drug Disco 9 (11) (2010) 883–897.
[25] T. Baumruker, A. Billich, V. Brinkmann, FTY720, an immunomodulatory sphingolipid mimetic: translation of a novel mechanism into clinical benefit in multiple sclerosis, Expert Opin. Invest. Drugs 16 (3) (2007) 283–289.
[26] N. Takasugi, et al., FTY720/fingolimod, a sphingosine analogue, reduces amyloid-β production in neurons, PloS One 8 (5) (2013), e64050.
[27] G. van Echten-Deckert, et al., Sphingosine-1-phosphate: boon and bane for the brain, Cell Physiol. Biochem 34 (1) (2014) 148–157.
[28] F. Hemmati, et al., Neurorestorative effect of FTY720 in a rat model of Alzheimer's disease: comparison with memantine, Behav. Brain Res 252 (2013) 415–421.
[29] K. Fukumoto, et al., Fingolimod increases brain-derived neurotrophic factor levels and ameliorates amyloid beta-induced memory impairment, Behav. Brain Res 268 (2014) 88–93.
[30] N. Aytan, et al., Fingolimod modulates multiple neuroinflammatory markers in a mouse model of Alzheimer's disease, Sci. Rep. 6 (2016) 24939.
[31] R. van Doorn, et al., Fingolimod attenuates ceramide-induced blood-brain barrier dysfunction in multiple sclerosis by targeting reactive astrocytes, Acta Neuropathol. 124 (3) (2012) 397–410.
[32] K.L. Youmans, et al., APOE4-specific changes in Abeta accumulation in a new transgenic mouse model of Alzheimer disease, J. Biol. Chem. 287 (50) (2012) 41774–41786.
[33] T.L. Stephen, et al., APOE genotype and sex affect microglial interactions with plaques in Alzheimer's disease mice, Acta Neuropathol. Commun. 7 (1) (2019) 82.
[34] S.M. Crivelli, et al., CERTL reduces C16 ceramide, amyloid-beta levels, and inflammation in a model of Alzheimer's disease, Alzheimers Res Ther. 13 (1) (2021) 45.
[35] R. Morris, Developments of a water-maze procedure for studying spatial learning in the rat, J. Neurosci. Methods 11 (1) (1984) 47–60.
[36] A. Blokland, E. Geraerts, M. Been, A detailed analysis of rats' spatial memory in a probe trial of a Morris task, Behav. Brain Res 154 (1) (2004) 71–75.
[37] A. Blokland, K. Rutten, J. Prickaerts, Analysis of spatial orientation strategies of male and female Wistar rats in a Morris water escape task, Behav. Brain Res 171 (2) (2006) 216–224.
[38] J. Prickaerts, et al., Transgenic mice overexpressing glycogen synthase kinase 3beta: a putative model of hyperactivity and mania, J. Neurosci.: Off. J. Soc. Neurosci. 26 (35) (2006) 9022–9029.
[39] S.M. Crivelli, et al., Ceramide analog [18F]F-HPA-12 detects sphingolipid disbalance in the brain of Alzheimer's disease transgenic mice by functioning as a metabolic probe, Sci. Rep. 10 (1) (2020) 19354.
[40] E.G. Bligh, W.J. Dyer, A rapid method of total lipid extraction and purification, Can. J. Biochem Physiol. 37 (8) (1959) 911–917.
41 M.M. Donners, et al., Cathepsin K Deficiency Prevents the Aggravated Vascular Remodeling Response to Flow Cessation in ApoE-/- Mice, PLoS One 11 (9) (2016), e0162595.
[42] E.P. van der Vorst, et al., Myeloid A disintegrin and metalloproteinase domain 10 deficiency modulates atherosclerotic plaque composition by shifting the balance from inflammation toward fibrosis, Am. J. Pathol. 185 (4) (2015) 1145–1155.
[43] C. Mencarelli, et al., Goodpasture antigen-binding protein/ceramide transporter binds to human serum amyloid P-component and is present in brain amyloid plaques, J. Biol. Chem. 287 (18) (2012) 14897–14911.
[44] W.J. Dixon, Analysis of extreme values, Ann. Math. Stat. 21 (1959) 488–506.
[45] A. Jahn-Eimermacher, I. Lasarzik, J. Raber, Statistical analysis of latency outcomes in behavioral experiments, Behav. Brain Res 221 (1) (2011) 271–275.
[46] M.M. Mielke, et al., Serum sphingomyelins and ceramides are early predictors of memory impairment, Neurobiol. Aging 31 (1) (2010) 17–24.
47 M.M. Mielke, et al., Serum ceramides increase the risk of Alzheimer disease: the Women's Health and Aging Study II, Neurology 79 (7) (2012) 633–641.
[48] A.N. Begum, et al., Women with the Alzheimer's risk marker ApoE4 lose Abeta-specific CD4(+) T cells 10-20 years before men, Transl. Psychiatry 4 (2014), e414.
[49] X.Y. Chua, et al., Immunomodulatory sphingosine-1-phosphates as plasma biomarkers of Alzheimer's disease and vascular cognitive impairment, Alzheimers Res Ther. 12 (1) (2020) 122.
[50] S. Guo, et al., Higher level of plasma bioactive molecule sphingosine 1-phosphate in women is associated with estrogen, Biochim Biophys. Acta 1841 (6) (2014) 836–846.
[51] N. Gaudreault, et al., ApoE suppresses atherosclerosis by reducing lipid accumulation in circulating monocytes and the expression of inflammatory molecules on monocytes and vascular endothelium, Arterioscler. Thromb. Vasc. Biol. 32 (2) (2012) 264–272.
[52] W. Cao, H. Zheng, Peripheral immune system in aging and Alzheimer's disease, Mol. Neurodegener. 13 (1) (2018) 51.

53 D. Gate, et al., Clonally expanded CD8 T cells patrol the cerebrospinal fluid in Alzheimer's disease, Nature 577 (7790) (2020) 399–404.
[54] Z. Aminzadeh, E. Parsa, Relationship between Age and Peripheral White Blood Cell Count in Patients with Sepsis, Int J. Prev. Med 2 (4) (2011) 238–242.
[55] B. Korin, et al., High-dimensional, single-cell characterization of the brain's immune compartment, Nat. Neurosci. 20 (9) (2017) 1300–1309.
[56] E. Zenaro, et al., Neutrophils promote Alzheimer's disease-like pathology and cognitive decline via LFA-1 integrin, Nat. Med 21 (8) (2015) 880–886.
[57] J.A. Siegel, G.E. Haley, J. Raber, Apolipoprotein E isoform-dependent effects on anxiety and cognition in female TR mice, Neurobiol. Aging 33 (2) (2012) 345–358.
[58] D.G. Amaral, The primate amygdala and the neurobiology of social behavior: implications for understanding social anxiety, Biol. Psychiatry 51 (1) (2002) 11–17.
[59] D.S. Liu, et al., APOE4 enhances age-dependent decline in cognitive function by down-regulating an NMDA receptor pathway in EFAD-Tg mice, Mol. Neurodegener. 10 (2015) 7.
60 de Wit, N.M., et al., *Altered Sphingolipid Balance in Capillary Cerebral Amyloid Angiopathy*. J Alzheimers Dis, 2016.
[61] Y. Mizutani, A. Kihara, Y. Igarashi, Mammalian Lass6 and its related family members regulate synthesis of specific ceramides, Biochem J. 390 (Pt 1) (2005), 263-71.
[62] E.L. Laviad, et al., Characterization of ceramide synthase 2: tissue distribution, substrate specificity, and inhibition by sphingosine 1-phosphate, J. Biol. Chem. 283 (9) (2008) 5677–5684.
[63] N.M. de Wit, et al., Astrocytic ceramide as possible indicator of neuroinflammation, J. Neuroinflamm. 16 (1) (2019) 48.
[64] A. Elsherbini, et al., Association of Abeta with ceramide-enriched astrosomes mediates Abeta neurotoxicity, Acta Neuropathol. Commun. 8 (1) (2020) 60.
[65] G. Dawson, J. Qin, Gilenya (FTY720) inhibits acid sphingomyelinase by a mechanism similar to tricyclic antidepressants, Biochem Biophys. Res Commun. 404 (1) (2011) 321–323.
[66] N. Marchesini, Y.A. Hannun, Acid and neutral sphingomyelinases: roles and mechanisms of regulation, Biochem. Cell Biol. 82 (1) (2004) 27–44.
67 R.W. Jenkins, D. Canals, Y.A. Hannun, Roles and regulation of secretory and lysosomal acid sphingomyelinase, Cell Signal 21 (6) (2009) 836–846.
[68] E.V. Berdyshev, et al., FTY720 inhibits ceramide synthases and up-regulates dihydrosphingosine 1-phosphate formation in human lung endothelial cells, J. Biol. Chem. 284 (9) (2009) 5467–5477.
[69] H. Jesko, et al., Fingolimod affects transcription of genes encoding enzymes of ceramide metabolism in animal model of Alzheimer's disease, Mol. Neurobiol. 57 (6) (2020) 2799–2811.
[70] I. Carreras, et al., Dual dose-dependent effects of fingolimod in a mouse model of Alzheimer's disease, Sci. Rep. 9 (1) (2019) 10972.
[71] L.M. Healy, J.P. Antel, Sphingosine-1-phosphate receptors in the central nervous and immune systems, Curr. Drug Targets 17 (16) (2016) 1841–1850.